Protein Electrochemistry

International Edition: DOI: 10.1002/anie.201500191
German Edition: DOI: 10.1002/ange.201500191

Microscale Crystals of Cytochrome *c* and Calixarene on Electrodes: Interprotein Electron Transfer between Defined Sites**

Róise E. McGovern, Sven C. Feifel, Fred Lisdat, and Peter B. Crowley**

Abstract: *The assembly of redox proteins on electrodes is an important step in biosensor development. Recently, p-sulfonato-calix[4]arene was shown to act as "molecular glue" for the assembly and crystallization of cytochrome c (cyt c). Electrochemical data are presented for microscale cyt c–calixarene crystals grown on self-assembled monolayers (SAM)-modified Au electrodes. The crystals were characterized by cyclic voltammetry and exceptionally high concentrations of electroactive cyt c were obtained. The peak currents were found to increase linearly with the square root of the scan rate, thus allowing an evaluation of the rate constant for electron self-exchange. This study revealed high electroactivity accompanied by fast interprotein electron transfer in crystals, which may have implications for the construction of novel bioelectronic devices.*

Cytochrome *c* (cyt *c*, 13 kDa) is a well-characterized redox protein[1–3] that is used extensively in biosensor construction.[4–7] Frequently, this involves immobilization of the cationic cyt *c* on gold electrodes bearing self-assembled monolayers (SAM) of densely packed anionic alkanethiols.[8,9] While electron transfer within a cyt *c* monolayer is diffusionless, some mobility in the adsorbed state is important for redox communication with partner enzymes.[10] Subtle rearrangement of the relative orientations of the proteins can affect the electron transfer rate.[10–12]

The typically low cyt *c* concentration in monolayers (ca. 10 pmol cm^{-2}) can limit the sensitivity of electrochemical detection.[13] Constructs with higher amounts of electrode-addressable protein are required for improved performance. The layer-by-layer adsorption technique is one route to obtain high protein concentrations on electrodes.[14–16] Heterogeneous multilayer assemblies have been generated on SAM-modified electrodes with cyt *c* and anionic "glues" such as polyaniline sulfonic acid (PASA), DNA, or silica nanoparticles.[16,17] Up to 15 electroactive layers of cyt *c* have been assembled with PASA (Figure 1) and the electrochemical response increased with the number of layers as a result of direct interprotein electron transfer.[16]

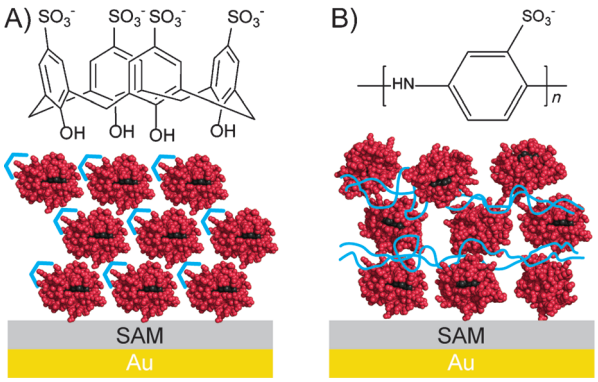

Figure 1. A) Cyt *c*–sclx$_4$ crystals are ordered assemblies with defined interheme distances. B) Cyt *c*–PASA multilayers are heterogeneous mixtures of protein–polymer contacts.

Protein crystals are the epitome of highly concentrated and ordered protein assemblies with potential biological relevance.[18] Although the assembled molecules lack rotational/diffusional mobility, there is strong evidence of electron transfer in redox protein crystals.[1,19–21] Knowledge of the separation distance between redox centers is useful for gauging interprotein electron transfer and so crystals are excellent model systems. Remarkably, so far there has been only one report of direct electrochemical characterization of protein crystals.[5] The immobilization of cyt *c* crystals in a polypyrrole film yielded cyclic voltammograms that were similar to those for standard cyt *c* monolayers.

p-Sulfonato-calix[4]arene (sclx$_4$) is a bowl-shaped molecular glue that is used for protein assembly and crystallization (Figure 1).[22,23] This calixarene shares some chemical properties with PASA. Notably, similar charge–charge interactions between the polyanion and the cationic cyt *c* drive protein complexation and assembly.[16,22] The key difference between the two systems is that the exact position of each protein is defined in the protein–small molecule crystal formed with sclx$_4$, while the multilayer assembly formed with PASA

[*] Dr. R. E. McGovern,[+] Dr. P. B. Crowley
School of Chemistry, National University of Ireland Galway
University Road, Galway (Ireland)
E-mail: peter.crowley@nuigalway.ie
Dr. S. C. Feifel,[+] Prof. Dr. F. Lisdat
Biosystems Technology, Institute of Applied Life Sciences
Technical University of Applied Sciences
Hochschulring 1, 15745 Wildau (Germany)
E-mail: flisdat@th-wildau.de
[+] These authors contributed equally to this work.

[**] We acknowledge funding from NUI Galway (fellowship to R.E.M.), the Irish Research Council ("New Foundations" Scheme to P.B.C.), Science Foundation Ireland (grant 10/RFP/BIC2807 to P.B.C.), the Deutsche Forschungsgemeinschaft (grant DFG Li 706/7-1 to F.L.) and the European Cooperation in Science and Technology (COST Action TD1003). P. Kavanagh (NUIG) is acknowledged for helpful discussions.

Supporting information for this article is available on the WWW under http://dx.doi.org/10.1002/anie.201500191.

comprises a heterogeneous mixture of protein–polymer and protein–protein contacts.

In this study, cyt *c* was co-crystallized with $sclx_4$ on Au electrodes. Conditions were identified to ensure crystal stability for direct electrochemical characterization by cyclic voltammetry. The crystal coverage of the electrodes was quantified microscopically (Olympus software) and related to the electrochemical data. Electron transfer was found to occur through the crystal in a fashion similar to that in cyt *c*–PASA multilayers.[24] This proof-of-principle study demonstrates for the first time that the electron self-exchange properties of cyt *c* can be exploited for long-range electron transport in the solid state on electrodes.

The crystallization and electrochemical characterization of cyt *c* was performed on planar Au chip electrodes with three different surfaces: bare, SAM-modified, and SAM-modified plus a cyt *c* monolayer. Protein–$sclx_4$ crystals were grown directly on the different electrode surfaces by using the hanging drop vapor diffusion method (Figure S1 in the Supporting Information).[22] Protein crystals grew on all three surfaces. CV measurements were performed initially in 5 mM potassium phosphate at pH 7. The crystals grown on a cyt *c* monolayer were displaced from the electrode during transfer from the crystallization solution to the measuring buffer and could not be characterized. The crystals on bare Au electrodes were more stable but redox peaks were not detected. Only the Au–SAM electrodes yielded electroactive crystals (Figure S2A). However, the electroactivity decreased over time during repeated measurements. This loss of activity could be correlated with a loss of crystals by dissolution/displacement from the electrode surface as verified by microscopic analysis.

To improve the stability of the crystals for electrochemical assessment, an adapted cell solution was used, that corresponds to the protein crystallization solution[22] (24% PEG 4000, 50 mM NaCl, 100 mM $MgCl_2$, pH 7.0). The Au–SAM–crystal electrodes showed a significantly different behavior under these conditions compared to the previous conditions (Figure S2B). The amount of electroactive species on the electrode surface remained constant or increased after repeated scans. This result suggests first that sufficient crystal stability could be obtained and second that the electrochemical addressability of cyt *c* in the crystals requires several redox cycles for activation. This can be understood in terms of reorganization since the oxidation/reduction of cyt *c* is accompanied by ion uptake or release.

On the basis of these results, a more comprehensive electrochemical investigation was performed. Au–SAM–crystal electrodes were subjected to a scan rate dependency study (10–1000 $mV\,s^{-1}$). Prior to the measurements, photographs were taken of each electrode (e.g., Figure 2) and the surface coverage of the crystals was determined (Table S1 in the Supporting Information). Photographs were also taken after the experiments to assess the crystal stability.

Voltammograms for the Au–SAM–crystal electrodes at each scan rate show a pair of redox peaks characteristic of a single redox species on the electrode surface (Figure 3A). The formal potential (E_f) of the cyt *c* Fe^{2+}/Fe^{3+} couple in the crystals at 100 $mV\,s^{-1}$ ($E_f = 0.049 \pm 0.006$ V vs. Ag/AgCl) was

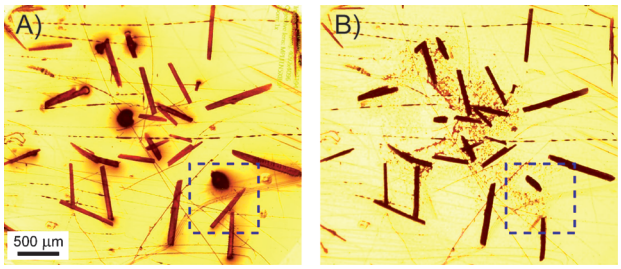

Figure 2. Region of a Au–SAM–crystal electrode before (A) and after (B) a scan rate dependency study. The highlighted area is an example of crystal dissolution/displacement. Note also the color change indicative of cyt *c* oxidation in (B). The SAM was prepared from mercaptoundecanol/mercaptoundecanoic acid (3:1).

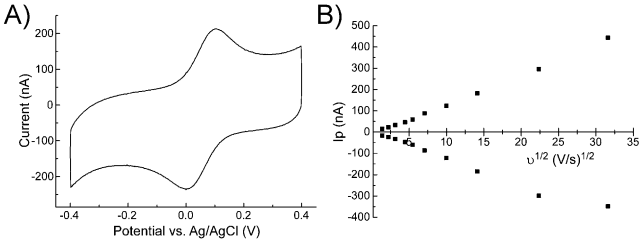

Figure 3. A) Cyclic voltammogram of a Au–SAM–crystal electrode at 100 $mV\,s^{-1}$. The cell solution was 24% PEG 4000, 50 mM NaCl, 100 mM $MgCl_2$, pH 7. B) Peak currents as a function of the square root of the scan rate.

slightly higher than the E_f value for a cyt *c* monolayer on a Au–SAM electrode measured at the same pH value ($E_f = 0.025 \pm 0.005$ V; Figure S3). This divergence between the two systems hints at minor alterations in the environment of the protein in the calixarene-containing crystals. The E_f varied only slightly with the scan rate and was consistent for the electrodes assessed (Table S2).

The anodic and cathodic peak currents for the redox couple increased linearly with the square root of the scan rate between 2 and 500 $mV\,s^{-1}$ (Figure 3B). This behavior can be rationalized in terms of electron hopping between defined positions within the crystal. The Randles–Sevcik equation[25] (see the Supporting Information) was used to determine an apparent "diffusion" coefficient for electron hopping between defined sites (rather than cyt *c* diffusion) and yielded a range of 10^{-9}–10^{-10} $cm^2\,s^{-1}$ (based on surface coverages of 0.1–0.5% for the different electrodes and a cyt *c* concentration of 55 mM in the crystal). These values are approximately two orders of magnitude larger than the diffusion coefficient in a cyt *c*–silica nanoparticle multilayer system (5×10^{-12} $cm^2\,s^{-1}$).[17] This result suggests that the ordered arrangement of the heme centers in the crystal is better suited to electron hopping than the heterogeneous multilayers with a distribution of cyt *c* orientations in the silica nanoparticle matrix.

Compared to a cyt *c* monolayer (Figure S3) the larger peak separation of the crystal electrode (Figure 3A, Table S2) suggests a slower rate of electron transfer (Figure S4). The increasing peak separation with scan rate originates from an

almost equal shift of the oxidation and reduction peak potentials, thus indicating similar kinetics for cyt *c* oxidation and reduction within the crystals. The half-peak-width value is larger than that for an ideal reversible system even at low scan rates and is typical of many protein electrodes.

The concentration of electroactive cyt *c* was determined for each electrode at the different scan rates. Although only a fraction of the electrode surface (< 1 %) was in contact with the crystals, an unprecedented amount of cyt *c* was detected (Table 1). This amount was dependent on the scan rate. At lower scan rates, larger amounts of protein contributed to the current. For example, an average electroactive cyt *c* concentration of 1200 pmol cm^{-2} was calculated at 1 V s^{-1}. This value increased approximately eight-fold when the scan rate was reduced to 2 mV s^{-1}, thus suggesting that electron transfer between protein layers in the crystals becomes rate limiting at higher sweep rates. The system cannot completely follow the fast change of electrode potential because the current depends on multiple electron self-exchange steps between the cyt *c* heme centers. This behavior is similar to cyt *c* multilayer electrodes, for which protein–protein electron transfer within the assembly is the main pathway and the limiting factor at higher scan rates.[16,17,24]

Table 1: Average values for the concentration of electroactive cyt *c* (Γ), E_f, and peak separation (ΔE_p) as a function of scan rate in three Au–SAM–crystal electrodes.

ν [mV s^{-1}]	1000	100	10	2
Γ [pmol cm^{-2}]	1200	2100	4500	9300
E_f [V vs. Ag/AgCl]	0.051	0.049	0.048	0.052
ΔE_p [V]	0.180	0.090	0.052	0.044

Microscopic analysis of the electrodes showed some displacement/dissolution of crystals after the CV study (Figure 2). Some electrodes gave even higher peak currents and hence higher concentrations of electroactive cyt *c* by the end of the measurement (Table S1). Therefore, two processes can apparently occur: dissolution of the crystals and "activation" of the crystals for electrochemistry. Importantly, the crystal dissolution or displacement was not pronounced during the timescale of our experiments. The "activation" may be connected with the large withdrawal or injection of electrons from/into the crystal and a concomitant reorganization of the counter ions in the crystal (to maintain electroneutrality).

In view of the crystal dissolution, it was essential to prove that the redox peaks corresponded to cyt *c* crystals and not to protein that had dissolved from the crystal. To assess this issue, a Au–SAM–crystal electrode was removed from the electrochemical cell after CV measurements and was replaced by a Au–SAM electrode lacking cyt *c*. The cell solution was not changed. Redox signals of dissolved cyt *c* were barely visible in the voltammogram (Figure S5). This verifies that the cyt *c* molecules in the crystals are the major contributors to the redox activity observed.

Redox activity in protein crystals has been characterized by various spectroscopic methods and electron transfer has been shown to occur when the cofactors are suitably positioned.[19–21] Here, we rationalized the electroactivity of the cyt *c*–sclx$_4$ crystals in terms of the heme–heme separation. Since the conditions used to grow cyt *c*–sclx$_4$ crystals on the electrodes were similar to those used for X-ray diffraction studies, the orientations of the cyt *c* molecules in the electroactive crystals were assumed to be identical to the crystal structure coordinates (PDB 4n0k, 1 Å resolution). The arrangement of the proteins in the crystal was determined by applying the $P2_12_12_1$ symmetry operations to the asymmetric unit (Figure 4).[22] Interestingly, the structure contains chains of cyt *c* molecules oriented "face-to-face" with Fe–Fe distances of 23.7 Å. This distance is compatible with long-range electron transfer, which according to Marcus theory occurs over distances less than 25 Å.[1] All other Fe–Fe distances in the crystal lattice were greater than 30 Å.

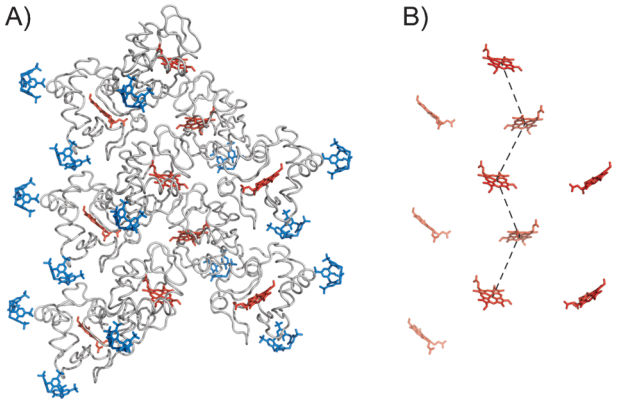

Figure 4. A) Cyt *c* arrangement in the calixarene-supported crystal[22] (PDB 4n0k). Cyt *c* is represented as a gray ribbon diagram with heme and sclx$_4$ as red and blue sticks, respectively. Crystal orientation is with the long axis of the unit cell parallel to the plane of the electrode. B) The shortest distance between Fe centers (23.7 Å) is indicated by dashed lines.

By using the interheme distances and the Randles–Sevcik diffusion coefficients (for electron hopping), we applied a modified Dahms–Ruff equation (see the Supporting Information) to estimate the self-exchange rate constant (k_{ex}) between the defined cyt *c* sites in the crystal. Values in the range of 10^5–10^6 M^{-1} s^{-1} were calculated, thus illustrating again the high efficiency of electron transport within the crystals.

In conclusion, high concentrations of cyt *c* were detected despite only a small area of the electrode (< 1 %) being in direct contact with protein crystals, thus suggesting that electron transport occurred through successive layers in the crystal. Similarities between these crystals and multilayer assemblies[16,17] were identified. The concentration of electroactive cyt *c* in the crystals was dependent on the scan rate, thus suggesting that the interprotein electron self-exchange rate becomes limiting at higher scan rates.[14,16] The electrode-addressable cyt *c* concentrations were one to two orders of magnitude larger than determined previously in cyt *c* multilayers.[16,24] This result is consistent with the greater thickness of the crystals compared to multilayer assemblies.

In addition to high protein concentrations, the advantage of the crystal system is that the precise positions and orientations of the redox centers are known. Molecular glues for protein assembly and crystallization[22,23] represent a new method for generating highly ordered protein architectures on electrodes. This approach might inspire the development of next-generation bioelectronic units that exploit protein–ligand interactions and mimick ET processes in nature.

Keywords: calixarenes · crystal growth · heme proteins · molecular glue · redox chemistry

How to cite: *Angew. Chem. Int. Ed.* **2015**, *54*, 6356–6359
Angew. Chem. **2015**, *127*, 6454–6457

[1] H. B. Gray, J. R. Winkler, *Biochim. Biophys. Acta Bioenerg.* **2010**, *1797*, 1563.
[2] A. N. Volkov, J. A. R. Worrall, E. Holtzmann, M. Ubbink, *Proc. Natl. Acad. Sci. USA* **2006**, *103*, 18945.
[3] C. Lange, C. Hunte, *Proc. Natl. Acad. Sci. USA* **2002**, *99*, 2800.
[4] E. Katz, A. F. Bückmann, I. Willner, *J. Am. Chem. Soc.* **2001**, *123*, 10752.
[5] F. Acosta, D. Eid, L. Marin-Gracia, B. A. Frontana-Uribe, A. Moreno, *Cryst. Growth Des.* **2007**, *7*, 2187.
[6] R. Dronov, D. G. Kurth, H. Möhwald, F. W. Scheller, F. Lisdat, *Angew. Chem. Int. Ed.* **2008**, *47*, 3000; *Angew. Chem.* **2008**, *120*, 3042.
[7] S. C. Feifel, R. Ludwig, L. Gorton, F. Lisdat, *Langmuir* **2012**, *28*, 9189.
[8] M. J. Tarlov, E. F. Bowden, *J. Am. Chem. Soc.* **1991**, *113*, 1847.
[9] S. Song, R. A. Clark, E. F. Bowden, M. J. Tarlov, *J. Phys. Chem. B* **1993**, *97*, 6564.
[10] W. Jin, U. Wollenberger, E. Krägel, W.-H. Schnuck, F. W. Scheller, *J. Electroanal. Chem.* **1997**, *433*, 135.
[11] A. Avila, B. W. Gregory, K. Niki, T. M. Cotton, *J. Phys. Chem. B* **2000**, *104*, 2759.
[12] A. Kranich, H. K. Ly, P. Hildebrandt, D. H. Murgida, *J. Am. Chem. Soc.* **2008**, *130*, 9844.
[13] B. Ge, F. Lisdat, *Anal. Chim. Acta* **2002**, *454*, 53.
[14] F. Wegerich, P. Turano, M. Allegrozzi, H. Möhwald, F. Lisdat, *Langmuir* **2011**, *27*, 4202.
[15] Y. Lvov, Z. Lu, J. B. Schenkman, X. Zu, J. F. Rusling, *J. Am. Chem. Soc.* **1998**, *120*, 4073.
[16] M. K. Beissenhirtz, F. W. Scheller, F. Lisdat, *Anal. Chem.* **2004**, *76*, 4665.
[17] S. C. Feifel, F. Lisdat, *J. Nanotechnol.* **2011**, *9*, 59.
[18] P. B. Crowley, P. M. Matias, H. Mi, S. J. Firbank, M. J. Banfield, C. Dennison, *Biochemistry* **2008**, *47*, 6583.
[19] B. R. Crane, A. J. Di Bilio, J. R. Winkler, H. B. Gray, *J. Am. Chem. Soc.* **2001**, *123*, 11623.
[20] S. A. Kang, B. R. Crane, *Proc. Natl. Acad. Sci. USA* **2005**, *102*, 15465.
[21] C. Cavalieri, N. Bierman, M. D. Vlasie, O. Einsle, A. Merli, D. Ferrari, G. L. Rossi, M. Ubbink, *Biochemistry* **2008**, *47*, 6560.
[22] R. E. McGovern, H. Fernandes, A. R. Khan, N. P. Power, P. B. Crowley, *Nat. Chem.* **2012**, *4*, 527.
[23] R. E. McGovern, A. A. McCarthy, P. B. Crowley, *Chem. Commun.* **2014**, *50*, 10412.
[24] M. K. Beissenhirtz, F. W. Scheller, W. F. M. Stöcklein, D. G. Kurth, H. Möhwald, F. Lisdat, *Angew. Chem. Int. Ed.* **2004**, *43*, 4357; *Angew. Chem.* **2004**, *116*, 4457.
[25] A. J. Bard, L. R. Faulkner in *Electrochemical Methods, Fundamentals and Applications*, Wiley-VCH, New York, **1980**.

Received: January 8, 2015
Published online: April 1, 2015

